European Journal of Radiology Open 2 (2015) 123–128

Contents lists available at ScienceDirect

European Journal of Radiology Open

journal homepage: www.elsevier.com/locate/ejro

IVIM diffusion-weighted imaging of the liver at 3.0 T: Comparison with 1.5 T

Yong Cui, Hadrien Dyvorne, Cecilia Besa, Nancy Cooper, Bachir Taouli*

Department of Radiology, Translational and Molecular Imaging Institute, Icahn School of Medicine at Mount Sinai, One Gustave Levy Place, New York, NY 10029, USA

ARTICLE INFO

Article history:
Received 3 June 2015
Received in revised form 21 August 2015
Accepted 22 August 2015
Available online 9 September 2015

Keywords:
Diffusion-weighted imaging
Intravoxel incoherent motion
3.0 T
Liver
Reproducibility

ABSTRACT

Purpose: To compare intravoxel incoherent motion (IVIM) diffusion-weighted imaging (DWI) of the liver between 1.5 T and 3.0 T in terms of parameter quantification and inter-platform reproducibility.
Materials and methods: In this IRB approved prospective study, 19 subjects (17 patients with chronic liver disease and 2 healthy volunteers) underwent two repeat scans at 1.5 T and 3.0 T. Each scan included IVIM DWI using 16 *b* values from 0 to 800 s/mm^2. A single observer measured IVIM parameters for each platform and estimated signal to noise ratio (eSNR) at *b*0, 200, 400 and 800 s/mm^2. Wilcoxon paired tests were used to compare liver eSNR and IVIM parameters. Inter-platform reproducibility was assessed by calculating within-subject coefficient of variation (CV) and Bland–Altman limits of agreement. An ice water phantom was used to test ADC variability between the two MRI systems.
Results: The mean invitro difference in ADC between the two platforms was 6.8%. eSNR was significantly higher at 3.0T for all selected b values ($p = 0.006$–0.020), except for *b*0 ($p = 0.239$). Liver IVIM parameters were significantly different between 1.5 T and 3.0 T ($p = 0.005$–0.044), except for ADC ($p = 0.748$). The inter-platform reproducibility of true diffusion coefficient (*D*) and ADC were good, with mean CV of 10.9% and 11.1%, respectively. Perfusion fraction (PF) and pseudodiffusion coefficient (*D**) showed more limited inter-platform reproducibility (mean CV of 22.6% for PF and 46.9% for *D**).
Conclusion: Liver *D* and ADC values showed good reproducibility between 1.5 T and 3.0 T platforms; while there was more variability in PF, and large variability in *D** parameters between the two platforms. These findings may have implications for drug trials assessing the role of IVIM DWI in tumor response and liver fibrosis.

1. Introduction

Diffusion weighted imaging (DWI) provides information about the functional environment of water in tissues by detecting the random microscopic motion of free water molecules known as Brownian motion. DWI of the liver has shown promise for tumor detection, characterization, for the prediction and assessment of response to therapy, and for detection of liver fibrosis and cirrhosis [1–5]. Intravoxel incoherent motion (IVIM) DWI separates diffusion and perfusion effects [6]. Because blood perfusion in chronic liver disease is an important surrogate marker for the severity of liver fibrosis [7], IVIM could be more sensitive than conventional DWI in characterizing liver fibrosis. Luciani et al. [8] used a 10 *b* values IVIM DWI sequence at 1.5 T and suggested that restricted diffusion observed in patients with cirrhosis were mainly related to decreased velocity of capillary blood [pseudodiffusion coefficient (*D**)]. These results were confirmed by Patel et al. [4], who additionally demonstrated that a significant decrease in liver static tissue molecular diffusion [true diffusion coefficient (D)], perfusion-related pseudodiffusion [perfusion fraction (PF) and pseudodiffusion coefficient (*D**)] in patients with cirrhosis when compared with subjects with noncirrhotic liver. Subsequently, similar results were reported by Dyvorne et al. [9]. Most of these previous IVIM DWI studies of liver were performed using 1.5T platforms. There is a growing interest in performing DWI at 3.0 T, which has the advantage of higher signal to noise ratio (SNR) compared to 1.5 T [10–13]. The effect of 3.0 T on quantitative diffusion parameters in the abdomen in comparison with 1.5 T has been rarely

Abbreviations: ADC, apparent diffusion coefficient; *D*, true diffusion coefficient; *D**, pseudo diffusion coefficient; DWI, diffusion-weighted imaging; IVIM, intravoxel incoherent motion.

* Corresponding author at: Icahn School of Medicine at Mount Sinai, Department of Radiology and Translational and Molecular Imaging Institute, One Gustave Levy Place, Box 1234, New York, NY 10029, USA. Fax: +1 212 427 8137.
E-mail address: bachir.taouli@mountsinai.org (B. Taouli).

http://dx.doi.org/10.1016/j.ejro.2015.08.001

described [14,15]. Rosenkrantz et al. [14] reported similar ADC values in the liver using 1.5 T and 3.0 T, while Dale et al. [15] reported significant field dependent differences in liver ADC. Knowledge of inter-platform variability in ADC and IVIM parameters may have implications for prospective drug trials assessing tumor response to therapy.

To our knowledge, there is no published comparison on the effects of field strength in liver IVIM parameters. This is important for the validation of quantitative diffusion metrics for response to therapy and for drug trials.

The purpose of this study was to compare 1.5 T and 3.0 T in terms of inter-platform variability in liver IVIM parameters.

2. Materials and methods

2.1. Phantom study

A phantom study was performed to test the calibration of ADC values at 1.5 T and 3.0 T. The phantom consisted of a center tube filled with distilled water surrounded by ice water, as described recently [16]. DWI sequence parameters are detailed in Table 1.

2.2. Subjects

This HIPAA compliant prospective study was funded by––and approved by our local Institutional Review Board. Informed signed consent was obtained from all participants. Seventeen patients with liver disease (M/F 12/5, mean age 58 y, range 30–69 y) were enrolled in the study from March 2012 to Jan 2013. Fourteen patients had viral hepatitis C and 3 had NASH. Liver fibrosis was proven by histopathology in 16 patients. In addition, 2 healthy volunteers (2 males, age 30 and 38 y) without history of liver disease were recruited for the study.

3. IVIM DWI

Each subject underwent two DWI scans, consisting of one scan on a 1.5 T platform (Magnetom Avanto, Siemens Healthcare) with a multichannel spine and body matrix coil and another scan on a 3.0T platform (Discovery MR 750; GE Healthcare) with a 32-channel phased array body coil (the same platforms were used for phantom study). The 1.5 T and 3.0 T scans occurred with a mean delay of 9 days (range, 0–45 days). All subjects were asked to fast for 6 h before the study. DWI acquisition was performed before contrast injection (in patients). A respiratory triggered (RT) DWI acquisition was used with a navigator at the 1.5 T (2D PACE: prospective acquisition correction, Siemens Healthcare) [17,18] and a free breathing DWI acquisition was used at 3.0 T (Table 1). DWI acquisition plane orientation was chosen according to the contrast imaging orientation of that subject. Axial acquisition was obtained at 3.0 T due to decreased distortion compared to coronal acquisition. Coronal acquisition was obtained in 13 subjects at 1.5 T, the rest having axial acquisition. Coronal orientation was chosen in order to match the coronal DCE-MRI acquisition in liver disease patients (not reported in this study).

3.1. Image analysis

3.1.1. Phantom data

An observer (observer 1—an MR physicist with 3 years of post-doctoral experience) reviewed DWI images of the phantom by using OsiriX (v.4.1.2, Pixmeo, Switzerland). An oval region of interest (ROI) of area 2 cm^2 was manually defined on the central slice through the central liquid water of the phantom to measure signal intensity (SI). ADC calculation was performed by least squares fitting of Eq. (1), where S_b is the signal intensity for each b value and S_0 is the signal intensity at a b value of zero:

$$\ln(S_b) = \ln(S_0) - b\mathrm{ADC}. \quad (1)$$

3.1.2. In vivo data

Another observer (observer 2—with 6 years experience in Body MRI) performed quantitative analysis of diffusion images. Five circular ROIs were placed manually within the right hepatic lobe on 5 consecutive slices centered on the main portal vein. The area of each ROI ranged from 6 to 9 cm^2. Care was taken to avoid large vessels and blurred regions in ROI placement. The left hepatic lobe was not assessed due to the possibility of cardiac motion artifacts. The same ROI mask was propagated to all b values. The DWI images of two scans (at 1.5 T and 3.0 T) for each subject were viewed simultaneously, with ROIs placed in as similar location as possible between scans. If the acquisition planes for one subject were different at two scans, measurements were done on coronally reformatted images of axial acquisition. Signal intensity (SI) of each pixel within each ROI was measured (Fig. 1), and the values of pixels within five ROIs (from five adjacent slices) were averaged for biexponential fitting. To examine the individual contributions of true molecular diffusion and incoherent motion of water molecules in the capillary network to the apparent diffusion changes, the mean SI in the ROI was fitted to the IVIM Eq. (2) (Fig. 1), where the SI decay with increasing b values as a fast pseudo-diffusion of constant D^* (pseudodiffusion coefficient) for the intravascular water fraction PF (perfusion fraction), and a slow molecular diffusion constant D (true diffusion coefficient), for the nonflowing spins [6]. SI_b is the signal intensity (SI) at an arbitrary b value. SI_0 is the SI in the absence of diffusion weighting ($b = 0$ s/mm^2).

$$SI_b = SI_0\{PFe^{-bD*} + (1 - PF)e^{-bD}\} \quad (2)$$

A Bayesian fitting method was used to estimate liver IVIM parameters [9,19]. The fitting method was implemented with in-house software programmed in Matlab (Matlab 2011a, MathWorks, Natick, MA, USA). In addition, mean liver ADC of each subject was obtained by using 16 b values of 0–800 s/mm^2 with mono-exponential least squares fit using Eq. (1). The mean ROI SI of each b value was used to fitting the ADC.

Finally, estimated signal-to-noise ratio (eSNR) was calculated for 4 selected b-values (0, 200, 400 and 800 s/mm^2) as follows: $eSNR = SI_{mean}/SD_{noise}$, where SI_{mean} is mean SI of all ROIs, SD_{noise} is standard deviation of background noise (measured on a small ROI outside the signal region).

3.2. Statistical analysis

SPSS 16.0 (SPSS Inc., Chicago, IL, USA) was used for all computations. A series of related samples Wilcoxon tests were used to compare eSNR, IVIM parameters and ADCs between 1.5 T and 3.0 T datasets. To evaluate inter-platform agreement of IVIM parameters and ADCs, the within-subject coefficient of variation (CV) and Bland–Altman limits of agreement were computed.

4. Results

4.1. Phantom study

The diffusion signal of the phantom showed a mono-exponential decay with increasing b values for each platform. The mean ADC values computed with 16 b values for 1.5 T and 3.0 T were 1.13 ± 0.03 and 1.21 ± 0.02 ($\times 10^{-3}$ mm^2/s), respectively. The mean difference of ADCs between the two platforms was 6.8%.

Table 1
Sequence parameters used for 1.5 T and 3.0 T IVIM DWI sequences.

Platform	1.5 T	3.0 T	1.5 T	3.0 T
Study type	In vivo		Phantom	
Acquisition plane	Coronal/Axial	Axial	Coronal	
Acquisition scheme	PACE	Free breathing	–	–
TR	1 respiratory cycle	2600	3000	2600
TE	74	59.5	74	58.3
b-Values (s/mm^2)	0, 15, 30, 45, 60, 75, 90, 105, 120, 135, 150, 175, 200, 400, 600, 800			
Diffusion directions	3			
Field of view (mm)	350–400			
Slice/interval thickness (mm)	8.0/1.6			
Number of slices	15	20–26	13	
Parallel imaging factor	2			
Number of averages	2	2	2	2
Acquisition matrix	160 × 128	128 × 128	160 × 128	128 × 128
Average scan time (min)	7–12	3:45	2:22	3:45

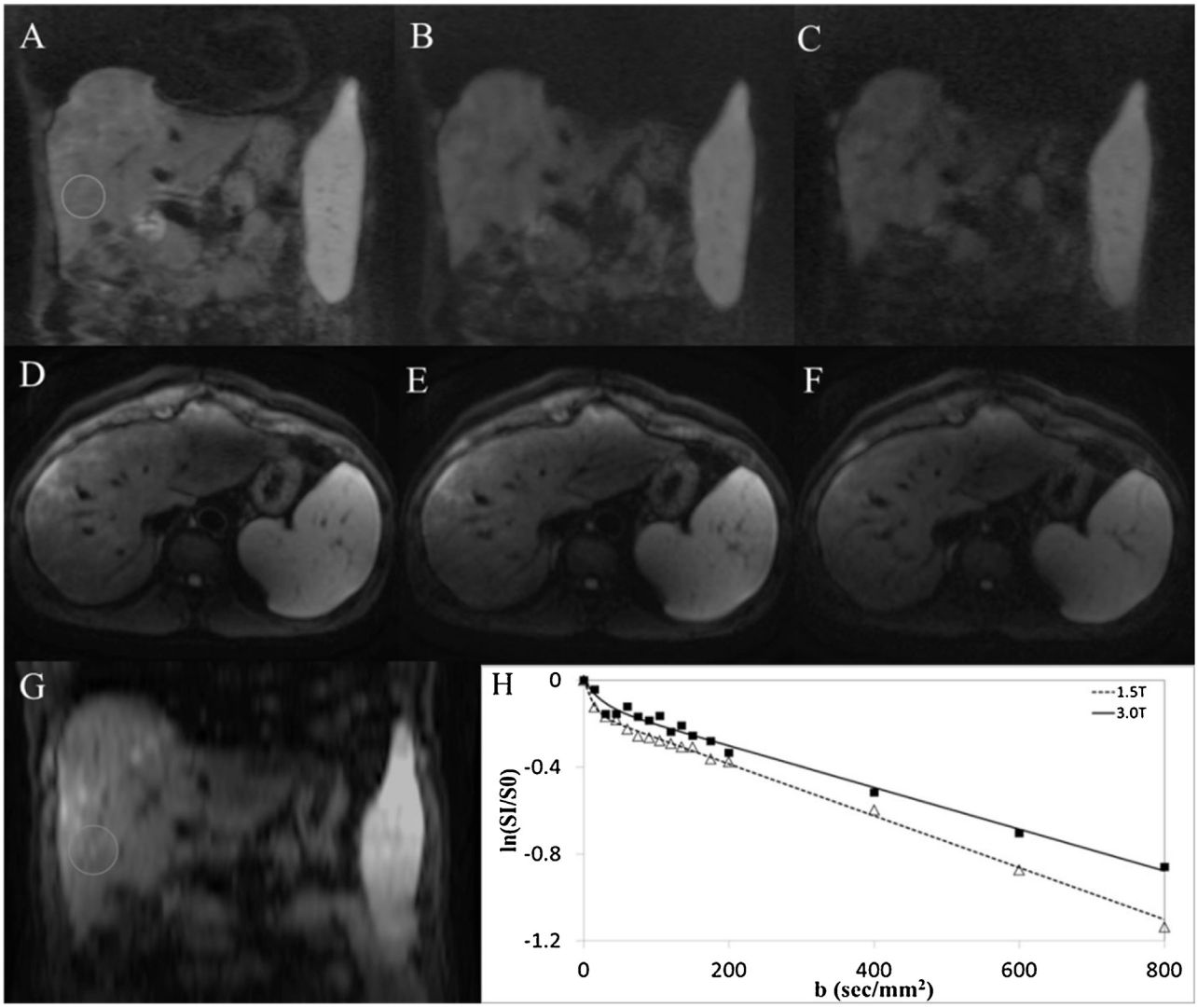

Fig. 1. 43-year-old male patient with HCV. SS EPI diffusion-weighted images acquired at 1.5 T and 3.0 T. (A–C): 1.5 T coronal DWI images [*b* = 200 (A), 400 (B), 800 (C)]. (D–F): 3.0T axial DWI images [*b* = 200 (D), 400 (E), 800 (F)]. (G): Coronal DWI image (*b* = 200) reformatted from axial acquisition at 3.0T. (A) and (G) show ROI placement for signal intensity measurement. ROIs with the same size were placed within the right hepatic lobes as similar location as possible between scans. (H): Graph shows liver SI decay with 16 *b* values acquired at 1.5 T (Δ) and 3.0 T (■). For display purposes, data were normalized to *b*0 SI. Dashed (1.5 T) and solid (3.0 T) lines are biexponential model curves using Bayesian estimated IVIM parameters Calculated values were *D* (true diffusion coefficient) = 1.19 and 0.96 × 10^{-3} mm^2/s, PF (perfusion fraction) = 13.6% and 10.4% and *D** (pseudo-diffusion coefficient) = 82.3 and 41.9 × 10^{-3} mm^2/s at 1.5 T and 3.0 T, respectively.

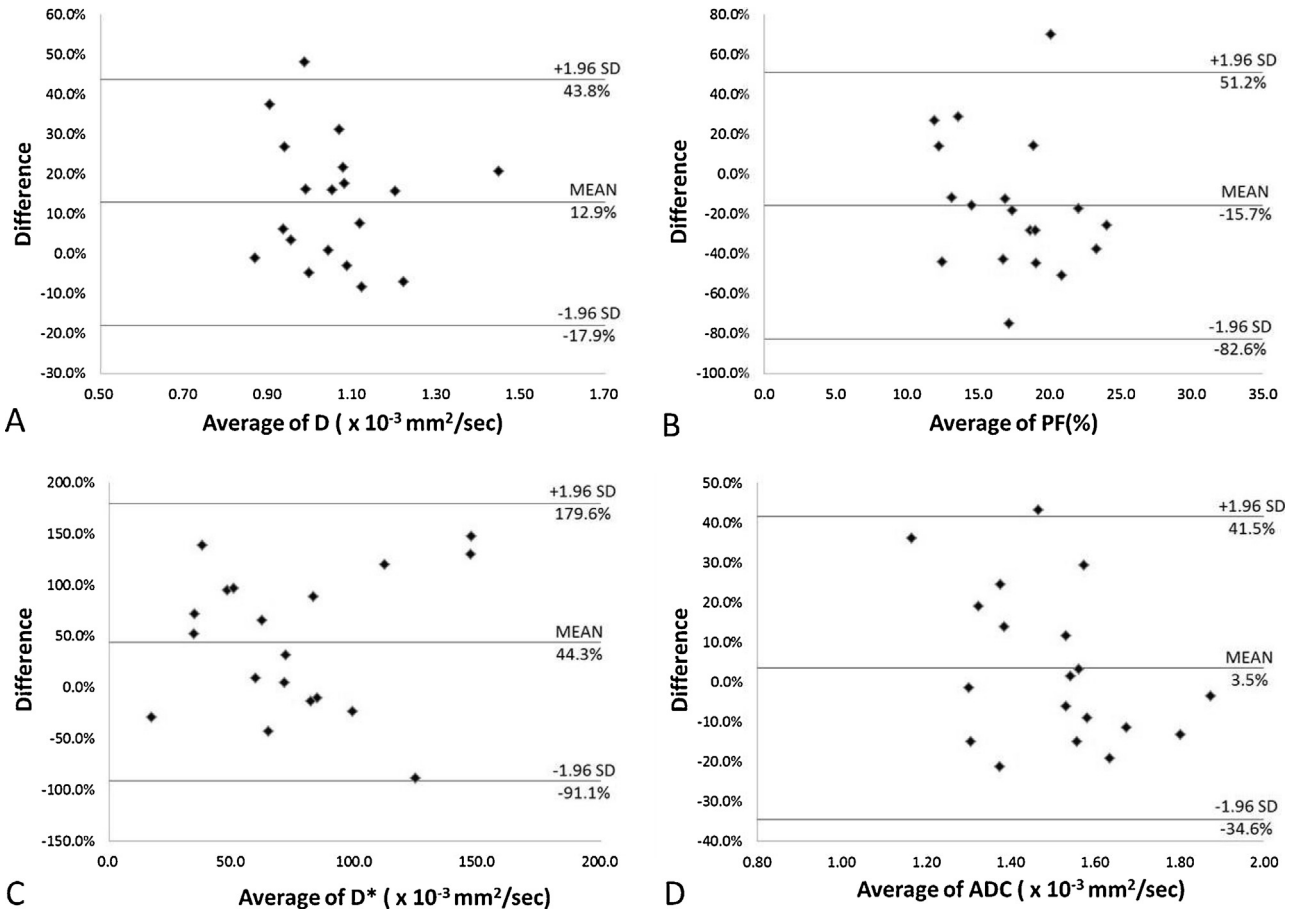

Fig. 2. Bland–Altman plots of percentage difference (*y*-axis) against mean (*x*-axis) of *D* (A), PF (B), *D** (C) and ADC (D) measurements at the 1.5 T and 3.0 T, with mean percentage difference and upper and lower limits of agreement (also refer to Table 3).

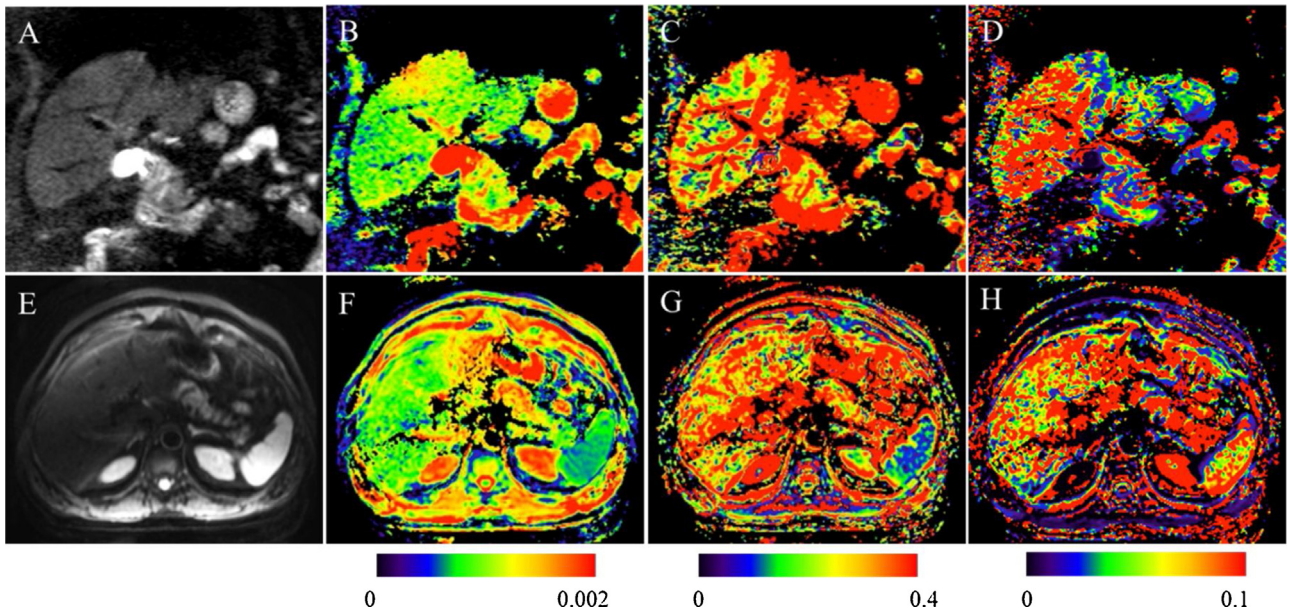

Fig. 3. 66-year-old male patient with HCV and Metavir stage 1 fibrosis. Parametric IVIM diffusion maps of the abdomen at 1.5 T (Coronal, A–D) and 3.0T (axial, E–H). A, E: SS EPI diffusion image (*b*200). (B and F): *D* map (true diffusion coefficient, mm^2/s). (C and G): PF map (perfusion fraction, %). (D and H): *D** map (pseudodiffusion coefficient mm^2/s). *D* maps show slightly higher values at the 1.5 T than the 3.0 T. *D** maps show higher values at the 1.5 T compared to the 3.0 T. PF maps show lower values at the 1.5 T compared to the 3.0 T. Calculated values were as follows: for *D*, 0.97 and 0.94×10^{-3} mm^2/s at the 1.5 T and the 3.0 T, respectively; for PF, 18.9% and 27.7%, respectively; for *D**, 82.9 and 60.3×10^{-3} mm^2/s, respectively.

Table 2
Estimated liver SNR of the 4 selected *b* value images acquired at 1.5 T and 3.0 T.

b value	1.5 T	3.0 T	*p*
*b*0	81.7 ± 65.7	93.5 ± 81.0	0.239
*b*200	55.6 ± 34.4	83.1 ± 69.9	0.020
*b*400	45.0 ± 30.4	69.1 ± 60.4	0.016
*b*800	29.5 ± 17.9	49.7 ± 39.8	0.006

Note: data are mean ± standard deviation.

4.2. In vivo study

There was a trend toward lower eSNR at increasing *b* values at both 1.5 T and 3.0 T. The eSNRs of DWI images at 3.0 T were higher compared to 1.5 T, reaching significance at $b = 200$, 400 and 800 but not at $b = 0$ (Table 2).

There were significant differences between platforms for *D* ($p = 0.005$), PF ($p = 0.033$) and D^* ($p = 0.044$). *D* and D^* were higher at 1.5 T compared to 3.0 T, while PF was lower at 1.5 T compared to 3.0 T. There was no significant difference in ADC between 1.5 T and 3.0 T ($p = 0.748$) **(**Table 3**)**.

The mean CVs between the two platforms varied from 10.9% to 46.9% (Table 3). Bland–Altman plots of the intra platform repeatability of IVIM parameters and ADC measurements for the liver parenchyma are shown in Fig. 2. A total of 94.7% (18/19) of data points were within the limits of agreement for each of the *D*, PF and ADC. All the data points (19/19) of D^* were within the limits of agreement. Fig. 3 shows examples of parametric maps at 1.5 T and 3.0 T.

5. Discussion

Recently, DWI has been increasingly investigated in the liver and has shown potential for the detection of liver fibrosis and cirrhosis [1,20,21] and for assessment of focal liver lesions [1,2,22]. With the advantage of separation of true diffusion from perfusion effects, IVIM DWI showed better diagnostic performance for detection of liver fibrosis [10,23]. Although these results indicated the potential of IVIM DWI as a quantitative tool of liver fibrosis, the widespread application of this method is still limited for lack of uniform acquisition and processing methods. It is difficult to get a reliable uniform criterion from results of different studies acquired with MR platforms at different field strengths without the knowledge of intra-platform reproducibility. Further validation of IVIM DWI comparability between different platforms—particularly quantitative assessment of the IVIM parameters is one of the major prerequisite for the IVIM parameters development as an imaging biomarker for liver fibrosis and for cancer drug trials.

The physical properties of water were well characterized previously [16,24]. In our study, to assess quantitative agreement across the two platforms, an ice water phantom study was applied first. The ADC value measured in our study for the ice water at 1.5 T was 1.13×10^{-3} mm^2/s, which was within 3% of the literature value of 1.1×10^{-3} mm^2/s [25], while the ADC value of ice water at 3.0 T in our study was 1.21×10^{-3} mm^2/s that was within about 9% of this value. These findings agree with previous published data [16], where 86% of the ice water ADC values obtained at 20 different human MRI scanners from three vendors were within 5% of the literature value and all measurements were within 10% of the value. Another recent study compared data from 35 clinical MRI systems form three vendors at 1.5 and 3.0 T, showed that multi-system reproducibility for ADC of ice water are within 2.8–3.1% [24] besides an outlier at 3.0 T with 70% higher than the literature value. The difference of ADC values between the two platforms was 6.8% in our study. These findings are close to those of Chenevert et al. [16], who showed that the variation of measured ADC values between all platforms tested was ±5%.

As a potential quantitative biomarker for liver fibrosis, inter platform reproducibility of IVIM is an important estimation of the reliability. In our study, the mean *D* of liver is 1.12×10^{-3} mm^2/s at 1.5 T and 0.99×10^{-3} mm^2/s at 3.0T. These findings lie within the range of previous published data, where the D value for liver fibrosis ranged from 1.02 to 1.19×10^{-3} mm^2/s at 1.5T [4,8,9] and 0.98 to 1.10×10^{-3} mm^2/s at 3.0 T [10]. The mean CV of the *D* values for fibrosis liver was 10.9% (range from 0.6% to 34.0%) between the 1.5 and 3.0 T platforms in our study. That is similar with the inter-platform reproducibility of the *D* values of fibrosis liver reported in previous studies [4,9], where mean CV ranged from 5% to 12.4%. Moreover, our study showed the inter-platform reproducibility was fair for PF (CV from 8.4% to 53.0%), and more limited for D^* (CV from 3.3% to 104.5%). Large differences in D^* may be attributed to fitting errors, as this parameter typically displays the largest fitting uncertainty in IVIM studies. Our study showed good reproducibility in liver ADC with mean CV of 11.1%. However, the application of ADC is not recommended, because it has been shown that the degree of signal attenuation of the liver with increasing *b* value is non-linear, the monoexponential fitting of ADC value is mathematically unacceptable except when *b* values are larger than 100–150 s/mm^2 [11]. Recent animal studies demonstrated an inverse relationship between *D* values and degree of liver fibrosis [26], and the *D* value can reflect the progression of liver fibrosis [23]. Taken together, these findings seem to imply the *D* value might be the most applicable and comparable parameter of IVIM DWI as a biomarker of liver fibrosis between different field strengths platforms.

Theoretically, the use of 3.0 T is ideal for DWI due to improved SNR compared to 1.5 T [13,27], as shown in our study. However, 3.0 T has also the disadvantages such as increased magnetic susceptibility artifact and eddy current related distortion [27]. In this context, qualitative analysis of artifacts and image distortions was often applied in previous field strength related study. Most of these studies showed that better DWI images were acquired at 1.5 T [14,28]. Because different acquisition plane orientations and breathing control techniques were used at the two platforms of our study, analysis of image quality was not applicable to our study.

Our study had some limitations. First, our study population was relatively small. Second, our study population consisted almost entirely of fibrosis patients, such as the utility of IVIM measurements for differential fibrosis liver from healthy subjects were not assessed. Third, different acquisition orientations and breathing control techniques were used at 1.5 T and 3.0 T in our study, which

Table 3
Liver IVIM parameters and ADC at 1.5 T and 3.0 T, with coefficients of variation (CVs) and Bland–Altman limits of agreement (BALA) between the two platforms.

Parameter	1.5 T	3.0 T	*p*	Mean CV (range, in%)	BALA (%)
D	1.12 ± 0.16	0.99 ± 0.16	0.005	10.9 (0.6 – 34.0)	−17.9, 43.8
PF	16.0 ± 4.1	19.0 ± 5.5	0.033	22.6 (8.4 – 53.0)	−82.6, 51.2
D^*	93.5 ± 64.0	57.2 ± 40.2	0.044	46.9 (3.3 – 104.5)	−91.1, 179.6
ADC	1.52 ± 0.18	1.48 ± 0.27	0.748	11.1 (1.0 – 30.5)	−34.6, 41.5

Note: data are mean ± standard deviation.
D, D^* and ADC: $\times 10^{-3}$ mm^2/s.
PF: %.

limited the application of qualitative image quality comparison between the two platforms. However, we focused on variability of quantitative parameters instead of image quality between platforms. Prior studies have reported good agreement between the ADCs acquired by different breathing control techniques DWI sequences [17,18]; with moderate to excellent parameter reproducibility for PF and D in IVIM of normal and fibrosis liver were found when different breath control technique applied [9]. Thus, we assumed that these difference acquisition protocols used in our study did not diminish the reliability of our results.

In conclusion, liver *D* and ADC values showed good inter-platform reproducibility between 1.5 T and 3.0 T. There was acceptable variability on PF, and large variability in D^* values between the two platforms. These findings may have implications for future drug trials and prospective studies assessing the role of DWI in tumor response and liver fibrosis.

Conflict of interest

None.

Acknowledgement

Grant support: NIDDK Grant 1R01DK087877.

References

[1] B. Taouli, D.M. Koh, Diffusion-weighted MR. imaging of the liver, Radiology 254 (2010) 47–66.
[2] N. Galea, V. Cantisani, B. Taouli, Liver lesion detection and characterization: role of diffusion-weighted imaging, J. Magn. Reson. Imaging 37 (2013) 1260–1276.
[3] A.R. Padhani, G. Liu, D.M. Koh, T.L. Chenevert, H.C. Thoeny, T. Takahara, et al., Diffusion-weighted magnetic resonance imaging as a cancer biomarker: consensus and recommendations, Neoplasia 11 (2009) 102–125.
[4] J. Patel, E.E. Sigmund, H. Rusinek, M. Oei, J.S. Babb, B. Taouli, Diagnosis of cirrhosis with intravoxel incoherent motion diffusion MRI and dynamic contrast-enhanced MRI alone and in combination: preliminary experience, J. Magn. Reson. Imaging 31 (2010) 589–600.
[5] B. Taouli, M. Chouli, A.J. Martin, A. Qayyum, F.V. Coakley, V. Vilgrain, Chronic hepatitis: role of diffusion-weighted imaging and diffusion tensor imaging for the diagnosis of liver fibrosis and inflammation, J. Magn. Reson. Imaging 28 (2008) 89–95.
[6] B. Le, D. ihan, E. Breton, D. Lallemand, P. Grenier, E. Cabanis, M. Laval-Jeantet, MR imaging of intravoxel incoherent motions: application to diffusion and perfusion in neurologic disorders, Radiology 161 (1986) 401–407.
[7] K.G. Hollingsworth, D.J. Lomas, Influence of perfusion on hepatic MR diffusion measurement, NMR Biomed. 19 (2006) 231–235.
[8] A. Luciani, A. Vignaud, M. Cavet, J.T. Nhieu, A. Mallat, L. Ruel, et al., Liver cirrhosis: intravoxel incoherent motion MR imaging—pilot study, Radiology 249 (2008) 891–899.
[9] H.A. Dyvorne, N. Galea, T. Nevers, M.I. Fiel, D. Carpenter, E. Wong, et al., Diffusion-weighted imaging of the liver with multiple *b* values: effect of diffusion gradient polarity and breathing acquisition on image quality and intravoxel incoherent motion parameters—a pilot study, Radiology 266 (2013) 920–929.
[10] J.H. Yoon, J.M. Lee, J.H. Baek, C.I. Shin, B. Kiefer, J.K. Han, et al., Evaluation of hepatic fibrosis using intravoxel incoherent motion in diffusion-weighted liver MRI, J. Comput. Assist. Tomogr. 38 (2014) 110–116.
[11] B. Guiu, J.M. Petit, V. Capitan, S. Aho, D. Masson, P.H. Lefevre, et al., Intravoxel incoherent motion diffusion-weighted imaging in nonalcoholic fatty liver disease: a 3.0-T MR study, Radiology 265 (2012) 96–103.
[12] J.H. Yoon, J.M. Lee, M.H. Yu, B. Kiefer, J.K. Han, B.I. Choi, Evaluation of hepatic focal lesions using diffusion-weighted MR imaging: comparison of apparent diffusion coefficient and intravoxel incoherent motion-derived parameters, J. Magn. Reson. Imaging 39 (2014) 276–285.
[13] K.J. Chang, I.R. Kamel, K.J. Macura, D.A. Bluemke, 3.0-T MR imaging of the abdomen: comparison with 1.5 T, Radiographics. 28 (2008) 1983–1998.
[14] A.B. Rosenkrantz, M. Oei, J.S. Babb, B.E. Niver, B. Taouli, Diffusion-weighted imaging of the abdomen at 3.0 Tesla: image quality and apparent diffusion coefficient reproducibility compared with 1.5 Tesla, J. Magn. Reson. Imaging 33 (2011) 128–135.
[15] B.M. Dale, A.C. Braithwaite, D.T. Boll, E.M. Merkle, Field strength and diffusion encoding technique affect the apparent diffusion coefficient measurements in diffusion-weighted imaging of the abdomen, Invest. Radiol. 45 (2010) 104–108.
[16] T.L. Chenevert, C.J. Galban, M.K. Ivancevic, S.E. Rohrer, F.J. Londy, T.C. Kwee, et al., Diffusion coefficient measurement using a temperature-controlled fluid for quality control in multicenter studies, J. Magn. Reson. Imaging 34 (2011) 983–987.
[17] B. Taouli, A. Sandberg, A. Stemmer, T. Parikh, S. Wong, J. Xu, et al., Diffusion-weighted imaging of the liver: comparison of navigator triggered and breathhold acquisitions, J. Magn. Reson. Imaging 30 (2009) 561–568.
[18] H. Kandpal, R. Sharma, K.S. Madhusudhan, K.S. Kapoor, Respiratory-triggered versus breath-hold diffusion-weighted MRI of liver lesions: comparison of image quality and apparent diffusion coefficient values, AJR Am. J. Roentgenol. 192 (2009) 915–922.
[19] J.J. Neil, G.L. Bretthorst, On the use of Bayesian probability theory for analysis of exponential decay data: an example taken from intravoxel incoherent motion experiments, Magn. Reson. Med. 29 (1993) 642–647.
[20] B. Taouli, A.J. Tolia, M. Losada, J.S. Babb, E.S. Chan, M.A. Bannan, et al., Diffusion-weighted MRI for quantification of liver fibrosis: preliminary experience, AJR Am. J. Roentgenol. 189 (2007) 799–806.
[21] R. Girometti, A. Furlan, G. Esposito, M. Bazzocchi, G. Como, F. Soldano, et al., Relevance of *b*-values in evaluating liver fibrosis: a study in healthy and cirrhotic subjects using two single-shot spin-echo echo-planar diffusion-weighted sequences, J. Magn. Reson. Imaging 28 (2008) 411–419.
[22] B. Taouli, V. Vilgrain, E. Dumont, J.L. Daire, B. Fan, Y. Menu, Evaluation of liver diffusion isotropy and characterization of focal hepatic lesions with two single-shot echo-planar MR imaging sequences: prospective study in 66 patients, Radiology 226 (2003) 71–78.
[23] A.M. Chow, D.S. Gao, S.J. Fan, Z. Qiao, F.Y. Lee, J. Yang, et al., Liver fibrosis: an intravoxel incoherent motion (IVIM) study, J. Magn. Reson. Imaging 36 (2012) 159–167.
[24] D. Malyarenko, C.J. Galban, F.J. Londy, C.R. Meyer, T.D. Johnson, A. Rehemtulla, et al., Multi-system repeatability and reproducibility of apparent diffusion coefficient measurement using an ice-water phantom, J. Magn. Reson. Imaging 37 (2013) 1238–1246.
[25] R. Mills, Self-diffusion in normal and heavy water in the range 1–45 deg, J. Phys. Chem. 77 (1973) 685–688.
[26] S.W. Anderson, H. Jara, A. Ozonoff, M. O'Brien, J.A. Hamilton, J.A. Soto, Effect of disease progression on liver apparent diffusion coefficient and T2 values in a murine model of hepatic fibrosis at 11.7 Tesla MRI, J. Magn. Reson. Imaging 35 (2012) 140–146.
[27] F. Springer, P. Martirosian, A. Boss, C.D. Claussen, F. Schick, Current problems and future opportunities of abdominal magnetic resonance imaging at higher field strengths, Top Magn. Reson. Imaging 21 (2010) 141–148.
[28] F. Saremi, M. Jalili, S. Sefidbakht, S. Channual, L. Quane, N. Naderi, et al., Diffusion-weighted imaging of the abdomen at 3 T: image quality comparison with 1.5-T magnet using 3 different imaging sequences, J. Comput. Assist. Tomogr. 35 (2011) 317–325.